The plant cytolytic protein enterolobin assumes a dimeric structure in solution

Silvia E.T. Bittencourt[a], Luciano P. Silva[b], Ricardo B. Azevedo[b], Ricardo B. Cunha[a,c], Consuelo M.R. Lima[a], Carlos A.O. Ricart[a], Marcelo V. Sousa[a,*]

[a] *Brazilian Center for Protein Research, Department of Cell Biology, University of Brasília, Brasília 70910-900, Brazil*
[b] *Laboratory of Morphology and Morphogenesis, Department of Genetics and Morphology, Institute of Biological Sciences, University of Brasília, Brasília 70910-900, Brazil*
[c] *Analytical Chemistry Area, Institute of Chemistry, University of Brasília, Brasília 70910-900, Brazil*

Received 7 May 2003; revised 25 June 2003; accepted 27 June 2003

First published online 16 July 2003

Edited by Marc Van Montagu

Abstract Enterolobin is a plant cytolytic protein similar to the bacterial cytolysin aerolysin. Biochemical and biophysical techniques were used to verify if enterolobin, like aerolysin, adopts a dimeric structure in solution. SDS–PAGE showed bands corresponding to enterolobin monomer, dimer and oligomers, whilst gel filtration chromatography and electrospray mass spectrometry revealed preferred association of enterolobin as a dimer. Atomic force microscopy (AFM) of enterolobin showed images of a dimer assembly at a concentration as low as 10 μg/ml, similarly to aerolysin. The enterolobin in silico docked structure is coherent with AFM enterolobin dimer shapes.

Key words: Pore-forming toxin; Plant protein; Enterolobin; Dimer; Quaternary structure; Atomic force microscopy

1. Introduction

Enterolobin is a cytolytic protein found in seeds of the Brazilian tree *Enterolobium contortisiliquum* [1]. Other activities such as insecticidal [2] and pro-inflammatory [3] ones are also present in the enterolobin molecule. The amino acid sequence of enterolobin shares 45% identity and 59% similarity with sequences of the bacterial cytolytic toxins named aerolysins found in *Aeromonas hydrophila* and other *Aeromonas* species [4,5].

Aerolysins exert their cytolytic action by pore formation on cell membranes [6]. Such pores are assembled after a multistep process which involves intracellular post-translational proteolytic maturation of pre-proaerolysin forming proaerolysin; secretion and extracellular proteolytic activation of proaerolysin leading to aerolysin; receptor binding and oligomerization of aerolysin on the target membrane [7]. The aerolysin heptamer assumes a channel shape with a hydrophylic interior and a hydrophobic external side. As proaerolysin, the toxin was shown to be stabilized by a dimeric quaternary assembly both in solution [8] and as a crystal [9]. Prior to oligomerization, a proteolytic activation is required to remove a C-terminal peptide. Conformational changes are then triggered, leading to dimer dissociation and receptor binding by activated aerolysin [7].

In this report, we show that enterolobin assumes a dimeric quaternary structure in solution like aerolysin. A number of methods such as SDS–PAGE, gel filtration, mass spectrometry and atomic force microscopy (AFM) were used to confirm the dimeric structure of the toxin.

2. Materials and methods

2.1. Materials

The seeds were harvested from *E. contortisiliquum* (Vell.) Morong trees in the region of Brasilia, Brazil, and kept in a cold room prior to use. Human red blood cells were drawn from healthy donors. All reagents and solvents were of analytical grade.

2.2. Enterolobin purification

Enterolobin purification was carried out according to a previously described method [5]. Hemolytic activity was determined in a microtiter plate assay using human red blood cells [1].

2.3. SDS–PAGE

Purified enterolobin was submitted to SDS–PAGE [10] using 7–15% polyacrylamide gradient gels. Prior to use, 10 μg of enterolobin was dissolved in sample buffer (0.32 M Tris–HCl pH 8.8, 1% (w/v) SDS, 12% (w/v) sucrose, 2% (v/v) 2-mercaptoethanol) and boiled for 5 min. The gels were stained by silver nitrate.

2.4. Gel filtration chromatography

The molecular mass of enterolobin was estimated by gel filtration chromatography using a FPLC apparatus fitted with a Superose 12 HR 10/30 column (Amersham Biosciences, Upsalla, Sweden). The column was previously equilibrated with TE buffer (50 mM Tris–HCl, 1 mM EDTA, 0.15 M NaCl, pH 9.0). The sample solution (2 mg of enterolobin/0.2 ml of TE buffer) was applied to the column at a flow rate of 0.5 ml/min. The absorbance was monitored at 280 nm. The molecular mass markers were thyroglobulin (670 kDa), bovine α-globulin (156 kDa), ovalbumin (44 kDa), horse myoglobin (17 kDa) and vitamin B12 (1.35 kDa). Blue Dextran 2000 (2000 kDa) was employed to determine the column void volume.

2.5. Mass spectrometry

Enterolobin was dissolved in water:isopropanol:formic acid (50:50:0.1) at a concentration of 5 pmol/μl, and injected into an electrospray triple quadrupole mass spectrometer (electrospray mass spectrometry (ES-MS)) Perkin Elmer-Sciex model API 300 (Ontario, Canada), equipped with a microionspray ionization probe, at a flow rate of 30 μl/h. The data were collected from *m/z* 200 to 2800, with 0.5 Da step size, 1 ms dwell time, 2 ms pause time and 30 scans. The raw data were processed and interpreted with the aid of BioMultiView version 1.2 from Perkin Elmer-Sciex.

*Corresponding author. Fax: (55)-61-273 4608.
E-mail address: mvsousa@unb.br (M.V. Sousa).

0014-5793/03/$22.00 © 2003 Published by Elsevier B.V. on behalf of the Federation of European Biochemical Societies.
doi:10.1016/S0014-5793(03)00763-4

2.6. AFM

For AFM analysis, enterolobin was diluted at a final protein concentration of 10 μg/ml in three different conditions: (a) Milli-Q water (H_2O-AFM); (b) 0.01% TFA (TFA-AFM); and (c) 300 mM KCl, 10 mM Tris–HCl, pH 7.4 (buffer-AFM). Four μl of each sample was deposited on freshly cleaved mica, and allowed to bind for 5 min. Preparations were then rinsed with 2–3 ml Milli-Q water, and partially air-dried. Samples were immediately imaged with a commercial AFM equipment (TopoMetrix Explorer TMX 2000, Santa Clara, CA, USA) operating in contact mode, following the conditions described in detail elsewhere [11]. Images were obtained in air, at room temperature, and at approximately 30% relative humidity. Scanned areas were perfect squares from 500 nm × 500 nm with 1 μm/s, applying a weak force (< 500 pN). All AFM images contained 500 × 500 data points, and the raw data images were processed and rendered with the aid of the software SPMLab 4.0 (TopoMetrix Explorer, Santa Clara, CA, USA). The reported lateral dimensions of surface features are the full width at half-maximum height. For presentation purposes, some images were processed by subtracting a general plane to remove the background slope.

2.7. Docking modeling

To determine potential sites of interaction between the monomers in order to form dimeric states of enterolobin, a homology-modeled structure of the molecule was built using the Geno3D software at http://geno3d-pbil.ibcp.fr [12] based on the proaerolysin PDB structure (1pre) as a template, and docked using the program GRAMM [13] at low resolution. PROCHECK was used to assess the homology model structural accuracy.

The docking procedure implemented an exhaustive grid search for the ligand–receptor structure matches. The docking parameters were: step of the grid, 6.8 Å; repulsion part of the potential, 6.5 Å; and interval for rotations, 20°. For each complex, the 1000 lowest-energy matches were analyzed. After a screening of possibilities, the best fit found was related to the lowest docking energy. Molecular structures were displayed by the RASMOL software package.

2.8. Protein volume calculations

The molecular volumes of the protein particles were measured by using the SPMLab software in two ways. In using the bearing analysis mode, the volumes of the molecular structures were measured from the top to the half-maximum height, and this value was doubled to obtain a corrected bearing volume.

The theoretical molecular volume based on molecular weight was calculated using Eq. 1 below:

$$V = (M_0/N_0)(V_1 + dV_2), \quad (1)$$

where M_0 is the protein's molecular mass, N_0 is Avogadro's number, V_1 and V_2 are the theoretical partial specific volumes of enterolobin and water (0.72 cm^3/g and 1 cm^3/g, respectively), and d is the extent of protein hydration (0.36 mol H_2O/mol protein). Theoretical partial specific volumes and hydration of enterolobin were determined by using the Sednterp software version 1.08 (Alliance Protein Laboratories, University of New Hampshire).

The molecular volumes based on PDB coordinates of modeled and docked molecules were determined by using Mark Gerstein's calcvolume program [14], in which the Normal Voronoi method with Richards's radii (1.4 Å) was employed.

All data were analyzed using ORIGIN 6.0 software (Microcal Software Inc., Northampton, MA, USA). AFM data were expressed as the mean ± S.D.

3. Results

Techniques as variable as SDS–PAGE, gel filtration and ES-MS were used to determine the molecular mass of enterolobin.

Initially, two well defined bands were revealed by SDS–PAGE of an enterolobin sample – its monomer at 52 kDa and a probable dimer at 94 kDa (Fig. 1). In addition, a broad band attributable to high mass oligomers stained on the top of the gel. Such an aggregation might be caused by SDS.

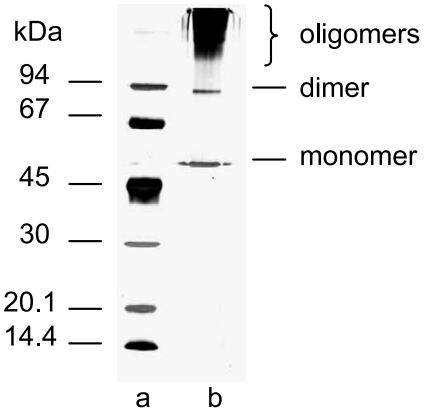

Fig. 1. SDS–PAGE of enterolobin. Gradient gels of 7–15% polyacrylamide were used. The gel was silver-stained. (a) Molecular mass markers. (b) Enterolobin (10 μg). Monomers, dimers and oligomers of enterolobin are indicated.

When analyses were made for enterolobin in solution, a dimeric protein structure was preferentially achieved. As for gel filtration chromatography in pH 9.0, a major peak at 109 kDa corresponding to enterolobin dimer was obtained (Fig. 2). No evident enterolobin monomer peak was observed in that experiment. Other peaks probably belonging to minor contaminant molecules showed molecular masses lower than 39 kDa.

Despite an inherent difficulty found to ionize enterolobin by ES-MS, such analysis also revealed a preferred association of enterolobin in a dimer arrangement. Molecular masses of 105 747.0, 106 995.0 and 107 034.0 Da were determined (Fig. 3), revealing possible enterolobin isoforms. This analysis was carried out at an acidic environment, as the spray solution had formic acid in its composition.

As a final way to probe the dimer formation of enterolobin, AFM was utilized. The protein was solubilized in three different solvents in order to assess the effect of pH on the dimer stabilization. The deposition protocol described in Section 2 led to mica–sample interactions strong enough to prevent

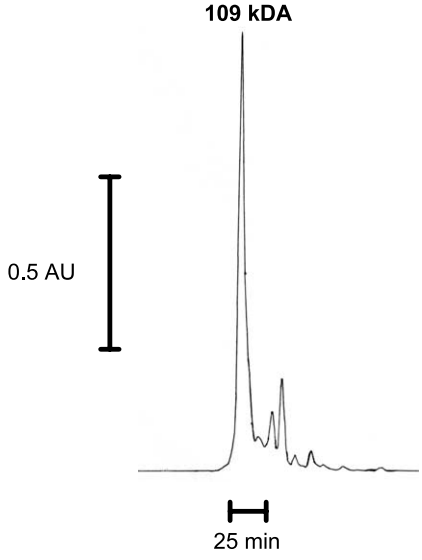

Fig. 2. Gel filtration of enterolobin. Two milligram of enterolobin dissolved in 0.2 ml of TE buffer was applied to a Superose 12 HR 10/30 column fitted to a FPLC. Flow rate was 0.5 ml/min. The absorbance was monitored at 280 nm.

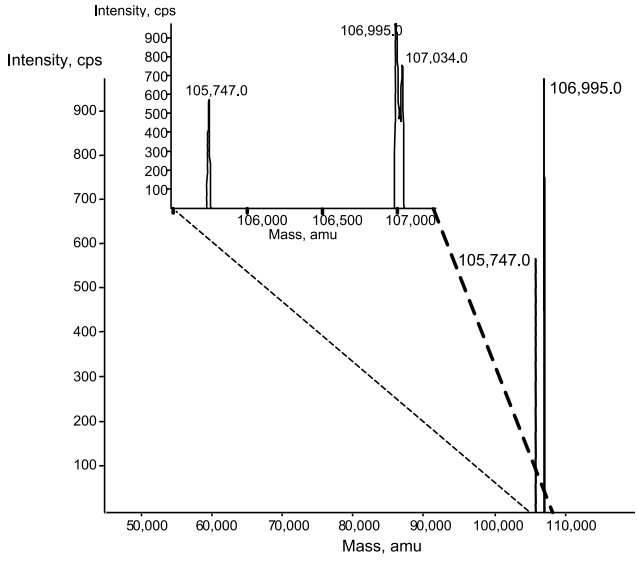

Fig. 3. ES-MS of enterolobin. Enterolobin spectrum was obtained with an electrospray triple quadrupole mass spectrometer. The protein was dissolved in water:isopropanol:formic acid (50:50:0.1) at a concentration of 5 pmol/μl. The reconstructed spectrum is shown with the molecular mass labels of protein peaks. The region of the enterolobin dimer is shown in a zoomed scale on the inset.

the tip from moving and sweeping the molecules around, but at the same time not too strong to cause deformation under water and buffer conditions (Fig. 4A,C). Under these conditions, enterolobin molecules were distributed as biconvex islands occupying approximately 5% of the mica total surface area. The noisy nature of AFM scans of enterolobin in TFA (Fig. 4B) indicates that proteins were adsorbed only weakly to the mica surface under this experimental condition, in spite of the fact that individual subunits appeared to be in a closer contact.

No convincing images of larger oligomers were found, and lateral aggregation was not observed under any conditions studied. For control experiments, Milli-Q water without protein was applied to a mica support and imaged after air-dried. Randomly distributed contaminations in control measurements were always less than 0.5 nm in height.

The homology model of enterolobin resulted in a deviation between model and template (rmsd) of 1.97 Å. The enterolobin subunits docked model fitted well with the AFM images for enterolobin dimers (Fig. 4). Enterolobin subunits consistently docked in a region that is similar to the previously determined X-ray crystallographic dimeric structure of the aerolysin (Fig. 4D,E), producing a structure resembling a handshake.

AFM-determined molecular volumes along 20 particles from enterolobin under each experimental condition were taken and compared with theoretical volumes and molecular docking models (coordinates) based volumes. We observed similar AFM volumes under all conditions, revealing a collective mean molecular volume of 111.36 ± 4.82 nm^3 (Table 1). This value is consistent with the enterolobin dimer when compared with theoretical volume prediction. The small discrepancy between these results and Voronoi volume measurement obtained from the lowest-energy dimer docked structure (14% higher) may be due to the model/docking inaccuracies.

4. Discussion

Data from SDS–PAGE (Fig. 1), gel filtration (Fig. 2) and ES-MS (Fig. 3) showed that enterolobin was likely to associate into dimers under a wide range of solvent and pH exposures. To confirm the hypothesis that enterolobin would really acquire such a dimeric structure, we submitted enterolobin solutions to AFM direct imaging. In three different conditions, we were able to obtain images showing a dimer assembly at a two-fold symmetry (Fig. 4A–C).

Previous results showed the predominance of monomer mass when enterolobin was analyzed by matrix-assisted laser desorption ionization/time-of-flight (MALDI-TOF) MS analysis [15]. Probably the harsher conditions of MALDI as compared to electrospray ionization can explain the difference between the results from the two MS ionization techniques. In fact, electrospray ionization is more suitable for protein quaternary structure studies, and has been more generally used for such a purpose.

The X-ray structure of proaerolysin, the precursor form of the pore-forming toxin aerolysin, showed it as a dimer in the crystal state [9]. In previous reports, both proaerolysin and aerolysin were shown to remain in the dimeric form in solution as determined by ultracentrifugation and chemical cross-linking followed by electrophoresis analyses [8]. It has also been demonstrated that proaerolysin folds and dimerizes before being released from the cell, and that correct folding is a requirement for secretion to occur [16].

More recently, an interesting discussion was initiated on whether proaerolysin would keep its dimeric structure at low concentrations. Fivaz et al. [17], using chemical cross-linking and gel filtration, argued that proaerolysin exists as a dimer only at a concentration above 100 μg/ml, but is monomeric at lower concentrations. According to them, dimer dissociation would precede cell receptor binding. On the other hand, Barry et al. [18], based on non-denaturing electrophoresis, chemical cross-linking and ultracentrifugation of proaerolysin, claimed that the protoxin is a dimer even at very low concentrations (less than 5 μg/ml), and that the dimer is capable of receptor binding. In the case of enterolobin, its dimeric structure was stable at concentrations as low as 10 μg/ml for AFM experiments. In this sense, our enterolobin results would agree with those of Barry et al. [18] for proaerolysin.

Since no experimentally determined 3D structure of entero-

Table 1
Volume (nm^3) analysis of enterolobin and proaerolysin dimers

	Theoretical volume	Voronoi volume	H_2O-AFM volume	TFA-AFM volume	Buffer-AFM volume
Enterolobin monomer	59.05	54.88	55.98 ± 4.39[a]	54.44 ± 2.53[a]	56.61 ± 2.87[a]
Enterolobin dimer	118.10	127.15	111.96 ± 5.55	108.88 ± 3.17	113.23 ± 4.88
Proaerolysin dimer	110.54	131.03	–	–	–

AFM data are expressed as the mean ± S.D.
[a]Monomer volume estimated by subunit segmentation on AFM topographic images.

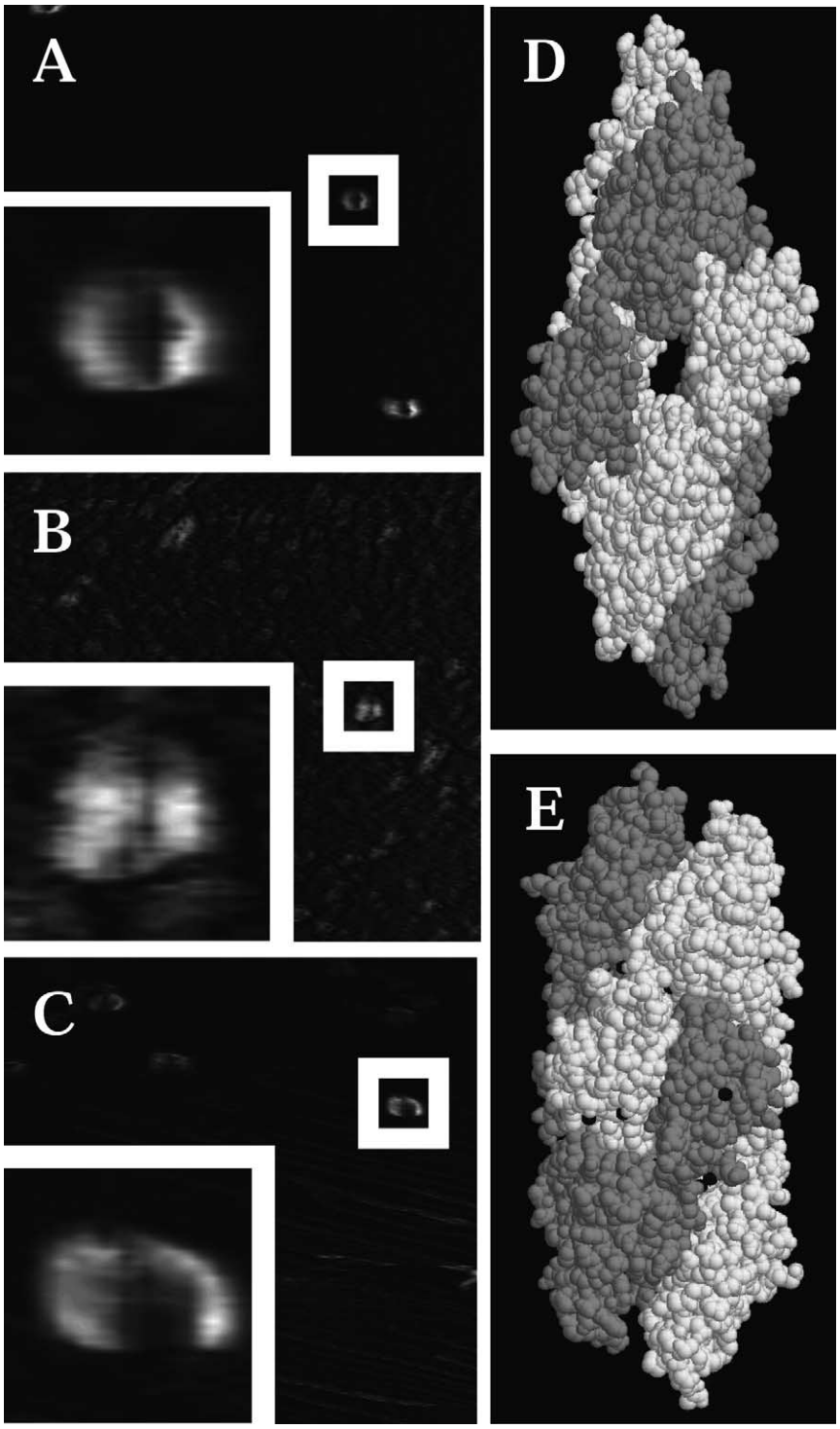

Fig. 4. AFM of enterolobin. Topographic AFM images of enterolobin molecules were taken under water (A), 0.01% TFA (B) and 300 mM KCl in 10 mM Tris–HCl, pH 7.4 (C). Insets show higher magnifications of the enterolobin structures. The major topographs had a full frame of 500 nm square and insets of 50 nm square. Full gray-level range of the topographs corresponds to 6.67, 6.54, and 6.47 nm for (A), (B), and (C), respectively. Space-filling molecular representations are depicted for the enterolobin docked dimer structure (D) and for the proaerolysin dimer (PDB code 1PRE) (E).

lobin exists yet, we used a molecular modeling approach associated with computational docking to compare an enterolobin dimer model with enterolobin dimer images obtained by AFM. The in silico enterolobin docked structure (Fig. 4D) is in agreement with the shape observed for the dimer on the AFM images (Fig. 4A–C), and were similar to that ones obtained from the crystal coordinate file of proaerolysin (Fig. 4E). Corroborating these qualitative observations, molecular volume approaches based on these experimental and theoretical results were quite similar (Table 1).

Taken together, the evidences points to a dimeric enterolobin structure in solution that remains stable at a concentration

as low as 10 μg/ml, similarly to aerolysin. Although there are fewer studies on enterolobin structure and function in comparison to aerolysin, it seems that enterolobin follows some molecular behavior that has been demonstrated for aerolysin, despite of the distant phylogenetic relationship between *Aeromonas* bacteria and the plant *E. contortisiliquum*.

Acknowledgements: The authors would like to thank Nuno Domingues for technical assistance on protein analytical methods. This work was supported by CNPq Grant no. 520279/95-6.

References

[1] Sousa, M.V. and Morhy, L. (1989) An. Acad. Bras. Ci. 61, 405–412.
[2] Sousa, M.V., Morhy, L., Richardson, M., Hilder, V.A. and Gatehouse, A.M.R. (1993) Entomol. Exp. Appl. 69, 231–238.
[3] Castro-Faria-Neto, H.C., Martins, M.A., Bozza, P.T., Perez, S.A., Correa-Da-Silva, A.C., Lima, M.C., Cruz, H.N., Cordeiro, R.S., Sousa, M.V. and Morhy, L. (1991) Toxicon 29, 1143–1150.
[4] Sousa, M.V., Richardson, M., Fontes, W. and Morhy, L. (1994) J. Protein Chem. 13, 659–667.
[5] Fontes, W., Sousa, M.V., Aragão, J.B. and Morhy, L. (1997) Arch. Biochem. Biophys. 347, 201–207.
[6] Bernheimer, A.W. and Avigad, L.S. (1974) Infect. Immun. 9, 1016–1021.
[7] Fivaz, M., Abrami, L., Tsitrin, Y. and Van der Goot, F.G. (2001) Toxicon 39, 1637–1645.
[8] Van der Goot, F.G., Ausio, J., Wong, K.R., Pattus, F. and Buckley, J.T. (1993) J. Biol. Chem. 268, 18272–18279.
[9] Parker, M.W., Bucley, J.T., Postma, J.P.M., Tucker, A.D., Leonard, K., Pattus, F. and Tsernoglou, D. (1994) Nature 367, 292–295.
[10] Laemmli, U.K. (1970) Nature 227, 680–685.
[11] Leite, J.R.S.A., Silva, L.P., Taveira, C.C., Teles, R.C.L., de Freitas, S.M. and Azevedo, R.B. (2002) Prot. Pept. Lett. 9, 179–184.
[12] Combet, C., Jambon, M., Deleage, G. and Geourjon, C. (2002) Bioinformatics 18, 213–214.
[13] Vakser, I.A., Matar, O.G. and Lam, C.F. (1999) Proc. Natl. Acad. Sci. USA 96, 8477–8482.
[14] Gerstein, M., Tsai, J. and Levitt, M. (1995) J. Mol. Biol. 249, 955–966.
[15] Lima, C.M.R., Grossi de Sá, M.F., Kalume, D.E., Roepstorff, P., Morhy, L., Ricart, C.A.O. and Sousa, M.V. (1999) J. Exp. Bot. 50, 1743–1750.
[16] Hardie, K.R., Schulze, A., Parker, M.W. and Buckley, J.T. (1995) Mol. Microbiol. 17, 1035–1044.
[17] Fivaz, M., Velluz, M.C. and Van der Goot, F.G. (1999) J. Biol. Chem. 274, 37705–37708.
[18] Barry, R., Moore, S., Alonso, A., Ausió, J. and Bucley, T. (2001) J. Biol. Chem. 276, 551–554.